



Platinum nanoparticles on nitrogen-doped carbon and nickel composites surfaces: A high electrical conductivity for methanol oxidation reaction



Geon-Hyoung An^a, Hyun-Gi Jo^b, Hyo-Jin Ahn^{a, b, *}

^a Program of Materials Science & Engineering, Convergence Institute of Biomedical Engineering and Biomaterials, Seoul National University of Science and Technology, Seoul 139-743, South Korea

^b Department of Materials Science and Engineering, Seoul National University of Science and Technology, Seoul 139-743, South Korea

ARTICLE INFO

Article history:

Received 23 February 2018

Received in revised form

15 May 2018

Accepted 25 May 2018

Available online 26 May 2018

Keywords:

Methanol oxidation reaction

Platinum

Nickel

Carbon supports

Dispersion

Electrical conductivity

ABSTRACT

Carbon has acquired considerable attention in view of its application as supports for platinum (Pt) catalyst in direct methanol fuel cells (DMFCs) with promising renewable energy source due to their high surface area and excellent chemical stability. However, the progress of carbon supports still needs to move towards the practical utilization of high-performance DMFCs. In the present study, we propose a novel support of nitrogen (N)-doped carbon and nickel (Ni) composites produced from protein using an impregnation process and carbonization to increase the electrical conductivity. To this end, we fabricated the Pt nanoparticles on N-doped carbon and Ni composites (Pt@NC/Ni). To obtain the optimized electrochemical performance, the amount of Ni components into carbon supports was controlled by three types. Specifically, as compared to commercial Pt/C and other samples, the optimized Pt@NC/Ni with the high electrical conductivity of 0.75 S cm^{-1} shows the lowest onset potential of 0.03 V, the highest anodic current density of $744 \text{ mA mg}_{\text{Pt}}^{-1}$, and an excellent catalytic stability with the highest retention rate of 86%. Accordingly, this novel support provides multiple advantages in terms of the well-dispersed Pt nanoparticles on the surface, N-doping effect of carbon supports, and an increased electrical conductivity by the introduction of Ni components. Therefore, Pt@NC/Ni is a promising novel catalyst to enhance electrochemical performance of methanol oxidation reaction.

© 2018 Elsevier B.V. All rights reserved.

1. Introduction

Depletion of fossil fuels and environmental pollution are critical challenges emerging due to the rapidly growing energy demand, which emphasizes the necessity to develop sustainable and clean energy sources [1,2]. Owing to their high energy densities, low operating temperatures, and ease of transportation and storage for long-term operation, direct methanol fuel cells (DMFCs) have attracted considerable attention as promising environmentally-friendly power sources [3–5]. In addition, with its principle of being renewable from biomass, the liquid type of methanol fuel is low cost and, as compared to pure hydrogen, has attractive advantages such as high solubility and excellent safety [6–8].

Notwithstanding, DMFCs still face the following two key barriers to successful commercialization: (1) expansive manufacturing costs due to high-cost precious platinum (Pt) catalyst; (2) slow kinetic rate of the methanol oxidation reaction (MOR) with Pt catalyst. Therefore, Pt nanoparticles as catalysts would be dispersed onto a carbon support to obtain a lot of electroactive sites between the catalyst surface and methanol fuel, leading to high-performance MOR [9–11]. Over the past decades, due to their due highly specific surface area, excellent chemical properties, environmental friendliness, and relative durability in electrolyte, carbon supports have been extensively investigated [1–5].

Many studies has sought to improve the performance of carbon supports. Of these strategies, the high surface area of carbon supports is an effective technique to obtain the well-dispersed Pt nanoparticles, leading to large electroactive sites [12–19]. Moreover, the introduction of nitrogen (N)-doping in carbon supports could act as an anchoring site for Pt nanoparticles deposited on its surface, resulting in an excellent electrochemical stability [20–22].

* Corresponding author. Department of Materials Science and Engineering, Seoul National University of Science and Technology, Seoul 139-743, South Korea.

E-mail address: hjahn@seoultech.ac.kr (H.-J. Ahn).

Furthermore, the relatively low electrical conductivity of carbon supports compared to metal supports remains an issue and is the reason for the limited electrochemical performance due to the slow electron transfer during MOR [4,5,16]. Thus, further progress of advanced carbon supports is still needed with regard to the practical utilization of high-performance DMFCs.

Thus, in the present study, we suggested the unique concept with the improvement of electrical conductivity by the introduction of nickel (Ni) component in a carbon support to improve electrochemical performance. In addition, the carbon support was fabricated from protein-based tofu, a traditional Asian food [23,24]. Due to its high carbon content and the presence of N, the protein consisting of amino acid is a powerful candidate as a raw material for functional carbon [23,24]. Hence, we fabricated Pt nanoparticles on N-doped carbon and Ni composites from protein and controlled the optimum amount of Ni component for the optimal catalysts for MOR.

2. Experimental

2.1. Chemicals

Protein from tofu (Pulmuone Co., Ltd.) was used. Nickel(II) chloride hexahydrate ($\text{NiCl}_2 \cdot 6\text{H}_2\text{O}$), chloroplatinic acid hydrate ($\text{H}_2\text{PtCl}_6 \cdot x\text{H}_2\text{O}$, $\geq 99.9\%$), nitric acid (HNO_3), hydrofluoric acid (HF), sodium borohydride (NaBH_4), Nafion perfluorinated resin solution, 2-propanol, methanol, and sulfuric acid (H_2SO_4) were purchased from Sigma-Aldrich.

2.2. Synthesis of Pt nanoparticles on N-doped carbon and Ni composites (Pt@NC/Ni)

The Pt nanoparticles on N-doped carbon and Ni composites (Pt@NC/Ni) were successfully fabricated using the impregnation process and carbonization. First, the protein-based tofu was prepared in the size of 1 cm^3 and then immersed in $\text{NiCl}_2 \cdot 6\text{H}_2\text{O}$ solution for 10 h. To optimize the Ni component, $\text{NiCl}_2 \cdot 6\text{H}_2\text{O}$ was gradually controlled using different amounts of 5, 10, 15 wt% $\text{NiCl}_2 \cdot 6\text{H}_2\text{O}$. To remove the solution, the impregnated sample was dried in an oven and heated at 300°C for stabilization. Afterwards, the ball-mill process was performed to acquire the nano-sized support. The carbonization was performed at 800°C under the nitrogen atmosphere. To invest the functional groups on the surface of the carbonized sample, the acid treatment was performed using a mixture (1:1 (v/v)) of HNO_3 and HF. To decorate the Pt nanoparticles on the surface, the reduction method was employed. A carbonized sample was dispersed in the $0.28\text{ mM H}_2\text{PtCl}_6 \cdot x\text{H}_2\text{O}$ solution and then reduced using the NaBH_4 solution (100 mg mL^{-1}) to load 10 wt% Pt nanoparticles on the surface. To obtain the metallic Pt phases, the resultant samples were acquired by the freeze-dry process under -50°C . Thus, we fabricated the three samples using different amounts of 5, 10, 15 wt% $\text{NiCl}_2 \cdot 6\text{H}_2\text{O}$ (thereafter referred to as Pt@NC/Ni 5, Pt@NC/Ni 10, and Pt@NC/Ni 15, respectively). For comparison, Pt nanoparticles on N-doped carbon without Ni component (thereafter referred to as Pt@NC) were synthesized. In addition, the commercial Pt/C (20 wt% Pt on carbon) was purchased from De Nora S.P.A. and further used for comparison.

2.3. Characterization

The structures and morphologies were explored by scanning electron microscopy (SEM) and transmission electron microscopy (TEM, KBSI Gwangju Center). X-ray diffractometry (XRD) in the range from 10° to 90° and X-ray photoelectron spectroscopy (XPS)

were used to investigate the crystal structures and chemical bonding states, respectively. The content of the samples was examined by the thermogravimetric analysis from 200 to 800°C at the heating rate of $10^\circ\text{C min}^{-1}$ in the air. To evaluate electrical conductivity, the prepared samples were coated on a glass substrate and measured using the hall measurement technique.

2.4. Electrochemical characterization

Electrochemical properties were investigated using a potentiostat/galvanostat in three-electrode system consisting of a glassy carbon (working electrode), a Pt wire (counter electrode), and an Ag/AgCl, sat. KCl (reference electrode). For the catalyst inks, the catalyst powder was dispersed in 2-propanol and deionized water containing Nafion solution. The catalyst ink was dropped on a glassy carbon and then dried in an oven. To identify the MOR, cyclic voltammograms (CV) was used between -0.2 and 1.0 V (vs. Ag/AgCl) at the scan rate of 50 mV s^{-1} in a $2\text{ M CH}_3\text{OH}$ and $0.5\text{ M H}_2\text{SO}_4$ electrolyte. To investigate the electrochemical stability, chronoamperometry (CA) was performed at the sustained potential of 0.5 V for 2000s, respectively. In addition, the long-term retention tests were performed using collecting CVs up to 7200 cycles. After the tests, the CV was repeatedly examined.

3. Results and discussion

The unique N-doped carbon and Ni composites was produced by the impregnation process and carbonization. First, the protein-based tofu was immersed in ethanol (Fig. 1a). To obtain the Ni component, 10 wt% $\text{NiCl}_2 \cdot 6\text{H}_2\text{O}$ was added (Fig. 1b). The impregnated protein was dried to remove the solution and then heated at 300°C for stabilization (Fig. 1c). N-doped carbon and Ni composite (Fig. 1d) as supports was obtained by the ball milling process and carbonization. Finally, Pt@NC/Ni 10, Pt nanoparticles on N-doped carbon and Ni composites (Fig. 1e) were successfully fabricated by the reduction method.

Fig. 2 shows the SEM images of Pt@NC (Fig. 2a), Pt@NC/Ni 5 (Fig. 2b), Pt@NC/Ni 10 (Fig. 2c), and Pt@NC/Ni 15 (Fig. 2d). The size of all samples with semi-block morphology ranged from ~ 150 to $\sim 395\text{ nm}$. In addition, all samples displayed smooth surfaces without aggregated nanoparticles, implying the well-dispersed Pt nanoparticles on the surface. To further investigate the structural characterization of the samples, the TEM measurements were also performed.

Fig. 3 shows low and high-magnification TEM images of Pt@NC (Fig. 3a and e), Pt@NC/Ni 5 (Fig. 3b and f), Pt@NC/Ni 10 (Fig. 3c and g), and Pt@NC/Ni 15 (Fig. 3d and h). Pt@NC (Fig. 3a and e) showed that Pt nanoparticles ($3\text{--}5\text{ nm}$) were dispersed on the surface without Ni component, indicating that the protein-based carbon was a favorable support for Pt nanoparticles. On the other hand, Pt@NC/Ni 5 (Fig. 3b and f), Pt@NC/Ni 10 (Fig. 3c and g), and Pt@NC/Ni 15 (Fig. 3d and h) showed well-dispersed Pt nanoparticles ($3\text{--}5\text{ nm}$) and Ni component into the N-doped carbon. The average size of Ni component for Pt@NC/Ni 5 and Pt@NC/Ni 10 ranged from 11 to 29 nm . In addition, the high-resolution TEM image of Pt@NC/Ni 10 (Fig. 3g) exhibited a clear lattice distance with the spacing of 0.22 nm and 0.34 nm , corresponding to the (111) planes of Pt and (002) planes of graphite. The Ni component into N-doped carbon could provide the formation of the graphite layer using catalytic action, leading to an improved electrical conductivity. However, Pt@NC/Ni 15 showed a large Ni component with the size range of $71\text{--}97\text{ nm}$, suggesting that the excessive amount of Ni was agglomerated in the N-doped carbon. To confirm the elemental distribution of Pt, Ni, C, and N of Pt@NC/Ni 10, the TEM-EDS mapping was performed (Fig. 3i). The obtained EDS data demonstrated

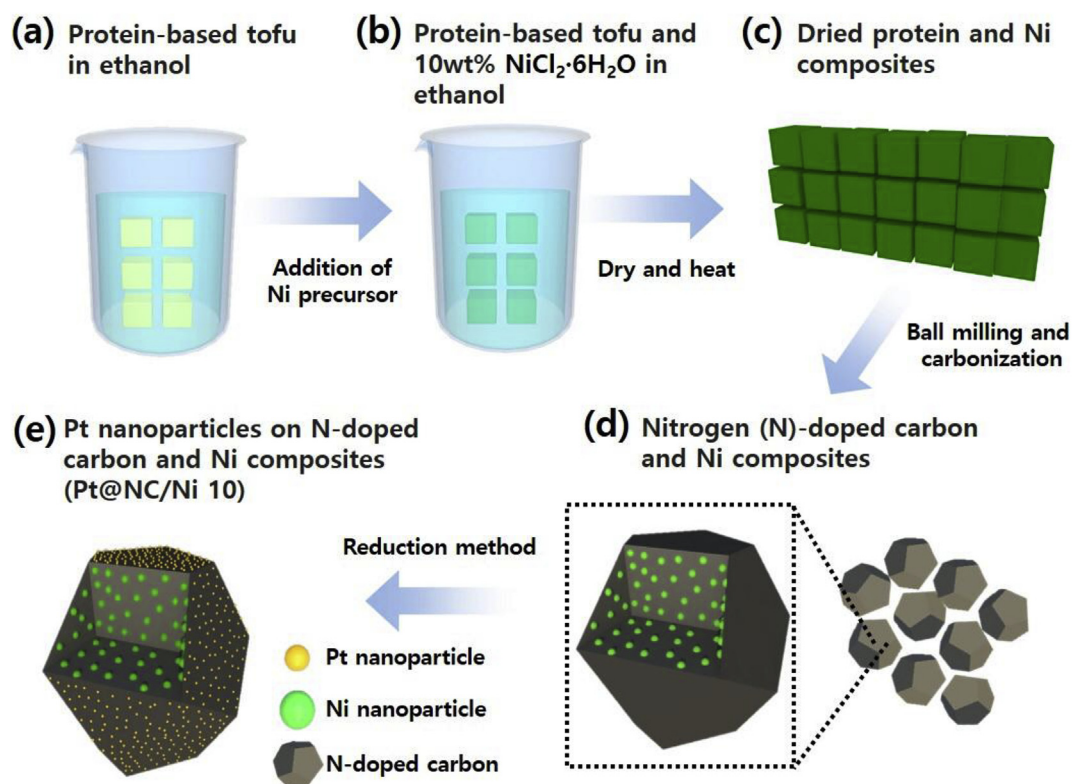


Fig. 1. Schematic illustration of the synthesis process for (a) protein-based tofu in ethanol, (b) protein-based tofu and 10 wt% NiCl₂·6H₂O in ethanol, (c) dried protein and Ni composites, (d) nitrogen (N)-doped carbon and Ni composites, and (e) Pt nanoparticles on N-doped carbon and Ni composites (Pt@NC/Ni 10).

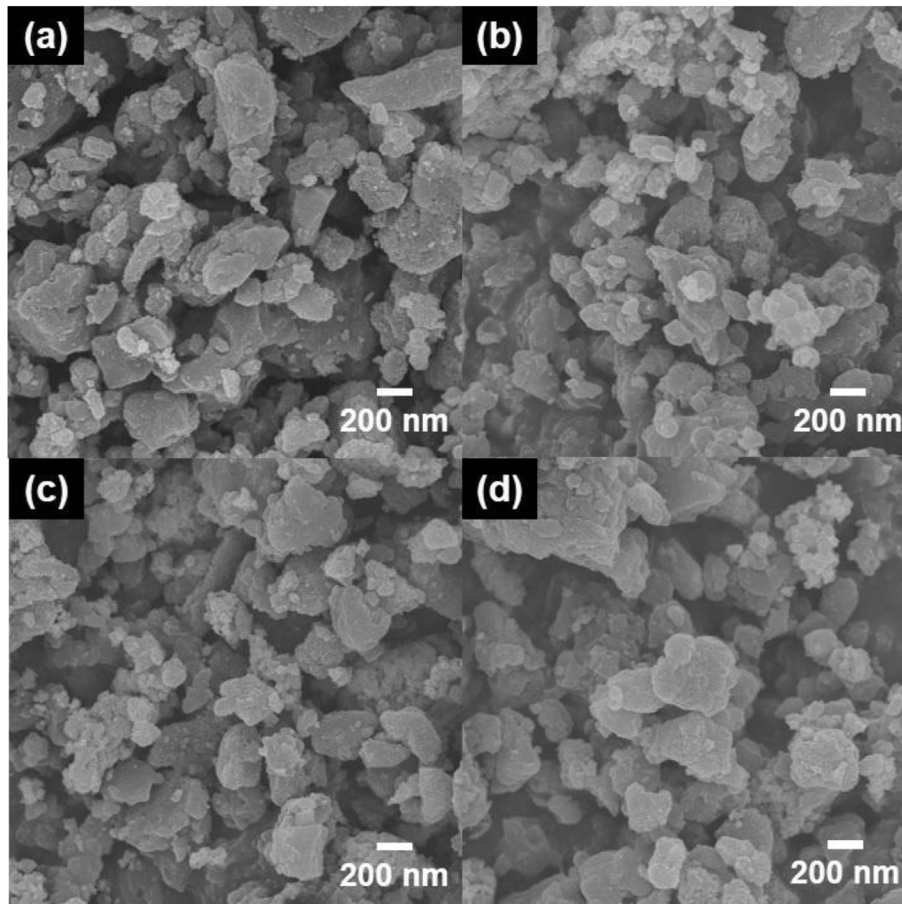


Fig. 2. SEM images of (a) Pt@NC, (b) Pt@NC/Ni 5, (c) Pt@NC/Ni 10, and (d) Pt@NC/Ni 15.

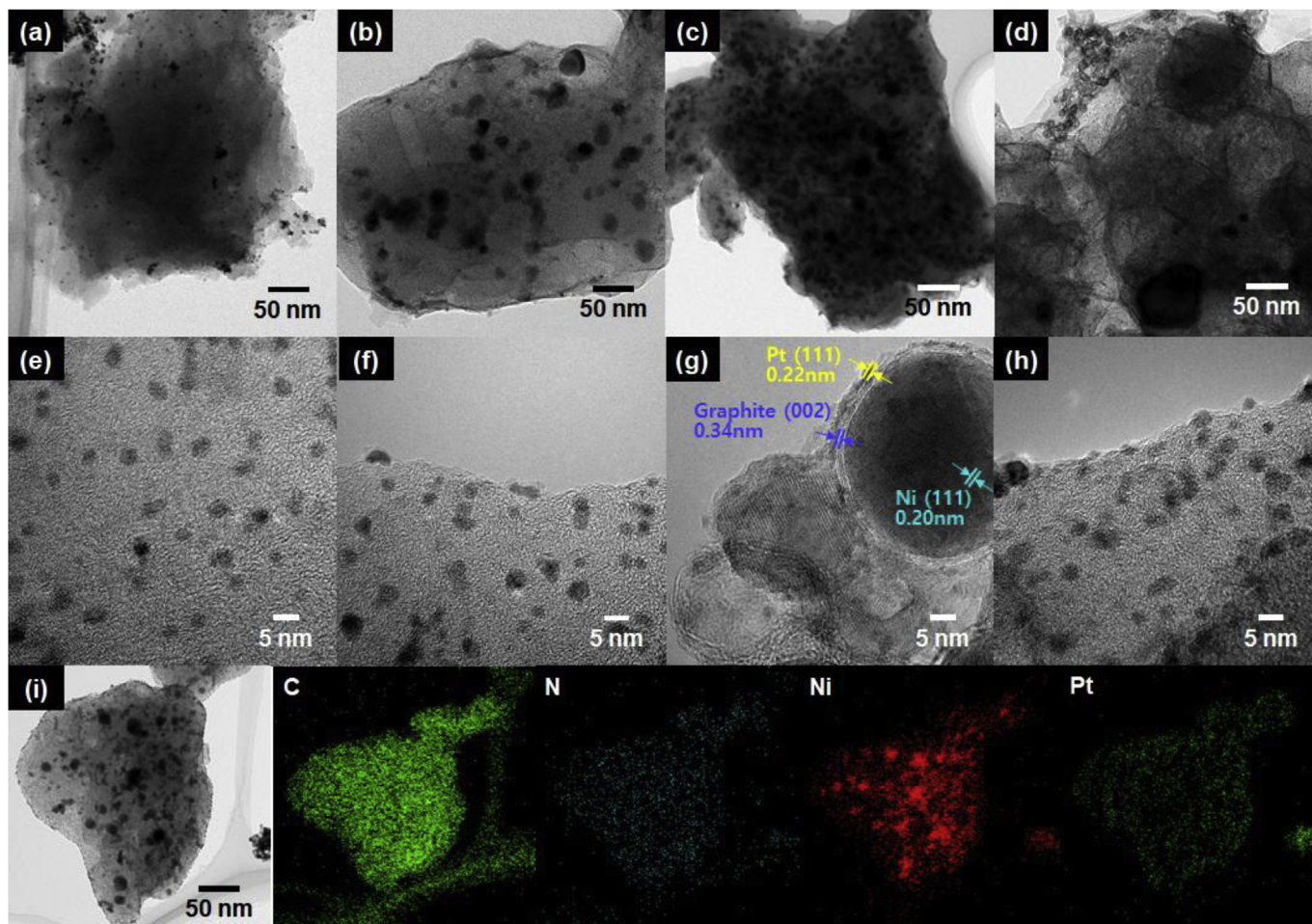


Fig. 3. (a–d) Low-resolution and (e–h) high-resolution TEM images of Pt@NC, Pt@NC/Ni 5, Pt@NC/Ni 10, and Pt@NC/Ni 15. (i) TEM-EDS mapping data of Pt@NC/Ni 10.

that the all elements were well distributed, with Ni components all embedded into the N-doped carbon and Pt nanoparticles well dispersed on the surface.

Fig. 4a shows the XRD data of Pt@NC, Pt@NC/Ni 5, Pt@NC/Ni 10, and Pt@NC/Ni 15 conducted to analyze the crystal structures. The diffraction peaks of pure Pt and pure Ni are indicated. The main diffraction peaks of Pt@NC, Pt@NC/Ni 5, Pt@NC/Ni 10, and Pt@NC/Ni 15 are observed at 39.7° , 46.2° , 67.5° , and 81.3° , corresponding to the (111), (200), (220), and (311) planes of metallic Pt phases with a face-centered structure, respectively [25]. In addition, Pt@NC/Ni 10, and Pt@NC/Ni 15 with a large amount of Ni components shows a diffraction peak at 44.5° , and 51.8° , corresponding to the (111) and (200) plane of metallic Ni phases with a face-centered structure, respectively [26,27]. The XPS measurements were performed to inspect the chemical state of Pt@NC/Ni 10 on the surface. The four types of C 1s spectra were C–C groups (284.5 eV), C–O groups (286.0 eV), C=O groups (287.6 eV), and O–C=O groups (288.7 eV), respectively [28–30] (Fig. 4b). Fig. 4c shows N 1s peaks in the XPS spectra. The decomposition of N was observed in four signals peaks at 398.4 eV, 400.0 eV, 401.0 eV, and 403.0 eV, corresponding to pyridinic-N, pyrrolic-N, graphitic-N, and pyridinic-N oxide, respectively [31]. The doped-N sites arose from the amino acid of the protein. Specifically, the pyridinic-N, including a pair of electrons in the plane of the carbon could provide one p-electron to the aromatic π -systems, leading to an increase of the electron-donor properties for catalytic performance. Therefore, the presence of pyridinic-N sites resulted in a marked improvement of

electrochemical activity [31]. The XPS spectra of Ni 2p were monitored at 855.7 eV and 862.1 eV, corresponding to nickel hydroxide and shake up satellites, respectively (Fig. 4d) [26,27]. The nickel hydroxide can be attributed to water vapor and O_2 in the air [26,27]. In addition, as shown in Fig. 4e, the XPS spectra of the metallic Pt phase were investigated at 72.3 eV and 75.4 eV.

To inspect the contents, the TGA measurement was used with the heating rate of $10^\circ\text{C min}^{-1}$ in the air from 200°C to 800°C (Fig. 5a). Pt@NC showed a weight loss of 90%, signifying the existence of Pt nanoparticles. In addition, as the relative amount of Ni component increased, the weight loss gradually increased as well. The weight loss of Pt@NC/Ni 5, Pt@NC/Ni 10, and Pt@NC/Ni 15 amounted to 77, 71, and 64%, respectively. In addition, the weight loss of NC/Ni 5, NC/Ni 10, and NC/Ni 15 without Pt nanoparticles amounted to 13, 19, and 26%, respectively (not shown). These results mean that the 10 wt% Pt nanoparticles were successfully fabricated on the composite supports. To investigate the effect of Ni component in carbon support, the electrical conductivity was measured by a hall measurement technique. Fig. 5b shows the electrical conductivities of Pt@NC, Pt@NC/Ni 5, Pt@NC/Ni 10, and Pt@NC/Ni 15. Of these, as compared to other samples, Pt@NC/Ni 10 exhibited highest electrical conductivity of 0.75 S cm^{-1} , implying the optimized amount of Ni components within well-dispersed Ni components in N-doped carbon supports. The increased electrical conductivity could efficiently improve the catalytic performance due to the improvement of electron transfer. On the other hand, owing to large aggregated Ni components in N-doped carbon

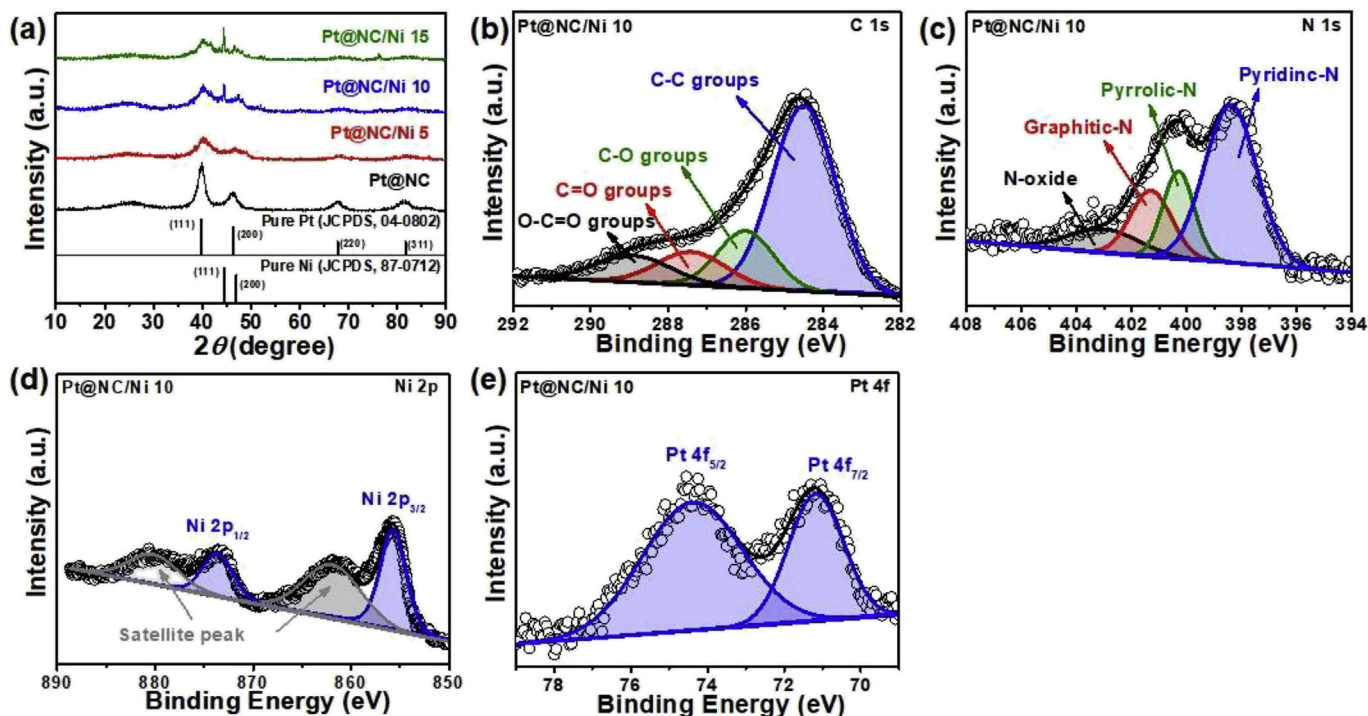


Fig. 4. (a) XRD patterns of Pt@NC, Pt@NC/Ni 5, Pt@NC/Ni 10, and Pt@NC/Ni 15. (b) C 1s, (c) N 1s, (d) Ni 2p, and (e) Pt 4f of Pt@NC/Ni 10.

support, Pt@NC/Ni 15 indicated a relatively low electrical conductivity of 0.47 S cm^{-1} . Moreover, the electrical conductivity of NC, NC/Ni 5, NC/Ni 10, and NC/Ni 15 without Pt nanoparticles is 0.1, 0.13, 0.39, and 0.21 S cm^{-1} respectively (not shown).

Fig. 6a shows the CV curves in a 2 M CH_3OH and 0.5 M H_2SO_4 electrolyte between -0.2 and 1.0 V (vs. Ag/AgCl) at the scan rate of 50 mV s^{-1} . The Pt loading mass was used to normalize the measured values. As is widely known, the MOR at the electrode generates 6 electrons, 6 protons, and carbon dioxide ($\text{CH}_3\text{OH} + \text{H}_2\text{O} \rightarrow 6\text{e}^- + 6\text{H}^+ + \text{CO}_2$) [9–11]. As the onset potential during MOR can demonstrate the catalytic performance. Pt@NC/Ni 10 exhibited the lowest onset potential of 0.03 V , suggesting the optimum amount of Ni component in N-doped carbon supports (Fig. 6a). All CV (Fig. 6b) curves present typical peaks, including methanol oxidation peak in the forward scan and intermediate species, such as CO, COOH, and CHO, in the backward scan. The value of methanol oxidation peak is

an important index in MOR. For the methanol oxidation peak of Pt@NC/Ni 10, the higher the number of electrons, the higher anodic current density as compared with other samples, signifying the enhanced electrochemical activity of MOR. Fig. 6c indicates that the anodic current densities of commercial Pt/C, Pt@NC, Pt@NC/Ni 5, Pt@NC/Ni 10, and Pt@NC/Ni 15 were 494, 510, 572, 744, and $639 \text{ mA mg}_{\text{Pt}}^{-1}$ in the forward scan at 0.65 V , respectively. The improved electrochemical activity of MOR can mainly be attributed to the high electrical conductivity of carbon supports resulting from the optimized amount of Ni components related to the improvement of electron transfer, as well as the well-dispersed Pt nanoparticles on the surface related to numerous electroactive sites.

The electrochemical stability and retention of MOR are critical parameters for use in practical applications of DMFCs. CA (Fig. 7a) was performed at 0.5 V for 2000s in a 2 M CH_3OH and 0.5 M H_2SO_4 electrolyte. The current densities of all samples were rapidly

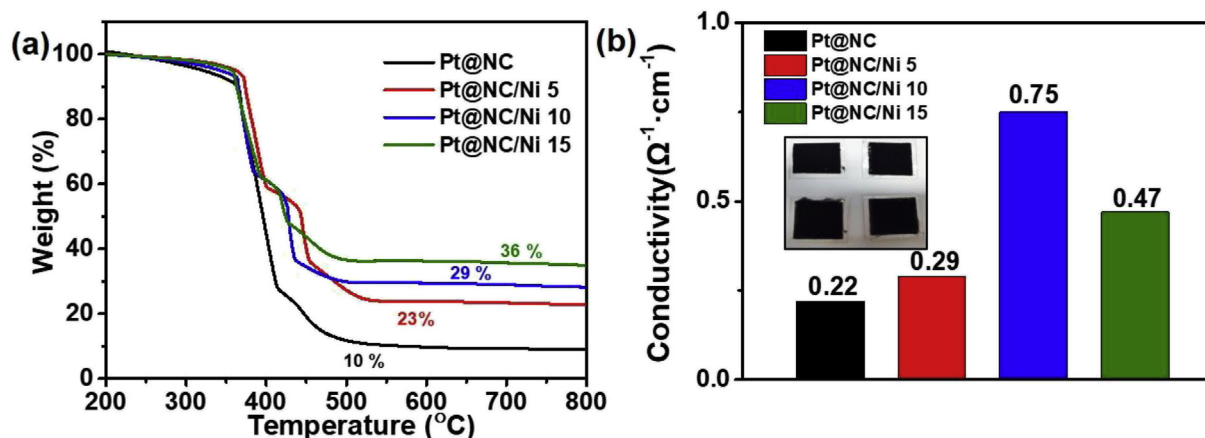


Fig. 5. (a) TGA curves and (b) electrical conductivities of Pt@NC, Pt@NC/Ni 5, Pt@NC/Ni 10, and Pt@NC/Ni 15.

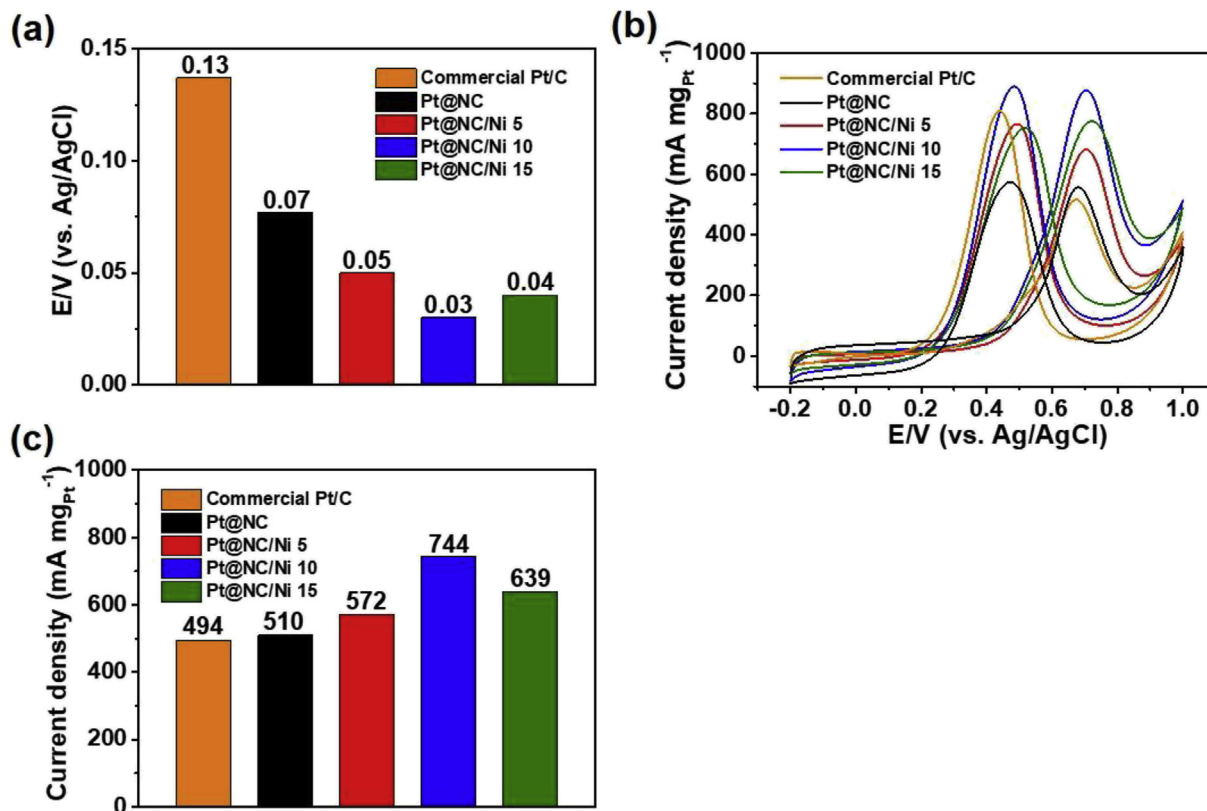


Fig. 6. Comparison of the catalytic activity of commercial Pt/C, Pt@NC, Pt@NC/Ni 5, Pt@NC/Ni 10, and Pt@NC/Ni 15. (a) On set potential in the forward scan. (b) Cyclic voltammetry (CV) measurements of methanol oxidation of commercial Pt/C, Pt@NC, Pt@NC/Ni 5, Pt@NC/Ni 10, and Pt@NC/Ni 15 at the scan rate of 50 mV s⁻¹ in the voltage range of -0.2–1.0 V. (c) Anodic current densities of all the samples at 0.65 V.

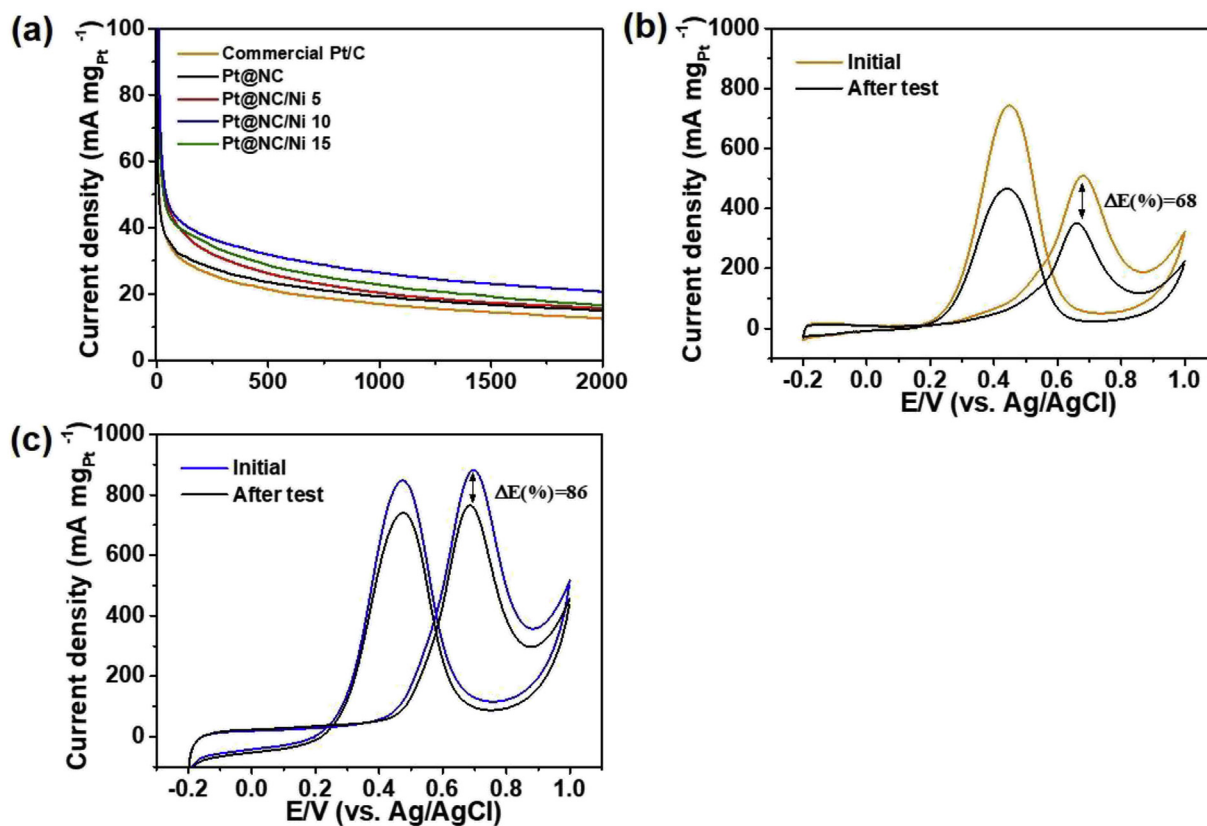


Fig. 7. (a) Chronoamperometry (CA) of commercial Pt/C, Pt@NC, Pt@NC/Ni 5, Pt@NC/Ni 10, and Pt@NC/Ni 15 in 0.5 M H₂SO₄ and 2 M CH₃OH electrolyte at 0.5 V. CV measurements after CA test of (b) commercial Pt/C and (c) Pt@NC/Ni 10, respectively.

reduced due to the adsorption of intermediate species and SO_4^{2-} anions onto the surface of Pt nanoparticles. Nonetheless, Pt@NC/Ni 10 showed the highest current density and the lowest deterioration rate, implying the excellent electrochemical stability. In addition, to investigate electrochemical retention, CA measurement was performed at 0.45 V in a 2 M CH_3OH and 0.5 M H_2SO_4 electrolyte for 7200s. Thereafter, the CV measurement was repeatedly run. CV curves of commercial Pt/C (Fig. 7b) and Pt@NC/Ni 10 (Fig. 7c) were obtained after the CA measurement, respectively. Pt@NC/Ni 10 presented the higher retention of 86% than commercial Pt/C (68%). Therefore, Pt@NC/Ni 10 displays the high current density and the high retention, suggesting that N-doping sites of carbon supports could efficiently help the electrochemical stability and retention using the synergistic interaction of Pt nanoparticles and carbon support [4,5,31].

4. Conclusions

In the present study, Pt@NC/Ni as a catalyst for MOR was successfully synthesized using the impregnation process and carbonization. The optimized Pt@NC/Ni 10 exhibited a novel structure for the well-dispersed Pt nanoparticles (3–5 nm) on the surface and an optimized amount of Ni components (11–29 nm) in the N-doped carbon supports. In addition, due to the optimized Ni components in N-doped carbon supports, Pt@NC/Ni 10 had the highest electrical conductivity of 0.75 S cm^{-1} as compared to other samples. Pt@NC/Ni 10 indicated an enhanced electrochemical performance with the lowest onset potential of 0.03 V, the highest anodic current density of $744 \text{ mA mg}_{\text{Pt}}^{-1}$, and an outstanding catalytic stability with the highest retention rate of 86% as compared to commercial Pt/C and other samples. The outstanding electrochemical performance can be attributed to the following two main factors: (i) the lowest onset potential and highest anodic current density are due to the optimized amount of Ni components well-dispersed Pt nanoparticles; (ii) the excellent catalytic stability is achieved due to the N-doping effect of carbon supports. Taken together, in terms of practical applications for DMFCs, the results of the present study indicate that the improved electrical conductivity of supports by Ni components and N-doping effect for Pt nanoparticles might be a key factor related to electron transfer.

Acknowledgments

This research was supported by Basic Science Research Program through the National Research Foundation of Korea (NRF) funded by the Ministry of Science, ICT and Future Planning (NRF-2015R1A1A1A05001252).

References

- [1] X. Shan, I.D. Perez, L. Wang, P. Wiktor, Y. Gu, L. Zhang, W. Wang, J. Lu, S. Wang, Q. Gong, J. Li, N. Tao, *Nat. Nanotechnol.* 7 (2012) 668–672.
- [2] M.K. Debe, *Electrocatalyst approaches and challenges for automotive fuel cells*, *Nature* 486 (2012) 43–51.
- [3] B.C.H. Steele, A. Heinzel, *Materials for fuel-cell technologies*, *Nature* 414 (2001) 345–352.
- [4] N. Kakati, J. Maiti, S.H. Lee, S.H. Jee, B. Viswanathan, Y.S. Yoon, *Anode catalysts for direct methanol fuel cells in acidic media: do we have any alternative for Pt or Pt-Ru*, *Chem. Rev.* 114 (2014) 12397–12429.
- [5] A.S. Arico, P. Bruce, B. Scrosati, J.M. Tarascon, W.V. Schalkwijk, *Nanostructured materials for advanced energy conversion and storage devices*, *Nat. Mater.* 4 (2005) 366–377.
- [6] Q.L. Wang, R. Fang, L.L. He, J.J. Feng, J. Yuan, A.J. Wang, *Bimetallic PdAu alloyed nanowires: rapid synthesis via oriented attachment growth and their high electrocatalytic activity for methanol oxidation reaction*, *J. Alloys Compd.* 684 (2016) 379–388.
- [7] Z. Wang, C. Lu, W. Kong, Y. Zhang, J. Li, *Platinum nanoparticles supported on core–shell nickel–carbon as catalyst for methanol oxidation reaction*, *J. Alloys Compd.* 690 (2017) 95–100.
- [8] I.A. Garcia, C. Ramirez, J.M.H. Lopez, E.M.A. Estrada, *Electrocatalytic activity of nanosized Pt alloys in the methanol oxidation reaction*, *J. Alloys Compd.* 495 (2010) 462–465.
- [9] G.H. An, E.H. Lee, H.J. Ahn, *Ruthenium and ruthenium oxide nanofiber supports for enhanced activity of platinum electrocatalysts in the methanol oxidation reaction*, *Phys. Chem. Chem. Phys.* 18 (2016) 14859–14866.
- [10] G.H. An, H.J. Ahn, W.K. Hong, *Electrochemical properties for high surface area and improved electrical conductivity of platinum-embedded porous carbon nanofibers*, *J. Power. Sources* 274 (2015) 536–541.
- [11] G.H. An, H.J. Ahn, *Pt electrocatalyst-loaded carbon nanofiber–Ru core–shell supports for improved methanol electrooxidation*, *J. Electroanal. Chem.* 707 (2013) 74–77.
- [12] X. Mu, Z. Xu, Y. Xie, H. Mi, J. Ma, *Pt nanoparticles supported on Co embedded coal-based carbon nanofiber for enhanced electrocatalytic activity towards methanol electro-oxidation*, *J. Alloys Compd.* 711 (2017) 374–380.
- [13] H. Gao, Y. Cao, Y. Chen, X. Lai, S. Ding, J. Tu, J. Qi, *Au nanoparticle-decorated NiCo₂O₄ nanoflower with enhanced electrocatalytic activity toward methanol oxidation*, *J. Alloys Compd.* 732 (2018) 460–469.
- [14] X. Li, M. Wen, D. Wu, Q. Wu, J. Li, *Pd-on-NiCu nanosheets with enhanced electro-catalytic performances for methanol oxidation*, *J. Alloys Compd.* 685 (2016) 42–49.
- [15] X. Hu, C. Ge, N. Su, H. Huang, Y. Xu, J. Zhang, J. Shi, X. Shen, N. Saito, *Solution plasma synthesis of Pt/ZnO/KB for photo-assisted electro-oxidation of methanol*, *J. Alloys Compd.* 692 (2017) 848–854.
- [16] M.A. Alvi, M.S. Akhtar, *An effective and low cost PdCe bimetallic decorated carbon nanofibers as electro-catalyst for direct methanol fuel cells applications*, *J. Alloys Compd.* 684 (2016) 524–529.
- [17] Y.-W. Lee, S.N. Cha, K.-W. Park, J.I. Sohn, J.M. Kim, *High performance electrocatalysts based on Pt nanoarchitecture for fuel cell applications*, *J. Nanomater.* 2015 (2015), 273720.
- [18] Y. Zhou, C. Zhu, G. Yang, D. Du, X. Cheng, J. Yang, Y. Lin, *Embedding platinum-based nanoparticles within ordered mesoporous carbon using supercritical carbon dioxide technique as a highly efficient oxygen reduction electro-catalyst*, *J. Alloys Compd.* 741 (2018) 580–589.
- [19] M. Du, B. Chen, Y. Hu, J. Chen, J. Nie, G. Ma, *Pt-based alloy nanoparticles embedded electrospon porous carbon nanofibers as electrocatalysts for Methanol oxidation reaction*, *J. Alloys Compd.* 747 (2018) 978–988.
- [20] X. Zhao, M. Yin, L. Ma, L. Liang, C. Liu, J. Liao, T. Lu, W. Xing, *Recent advances in catalysts for direct methanol fuel cells*, *Energy Environ. Sci.* 4 (2011) 2736–2753.
- [21] H. Liu, C. Song, L. Zhang, J. Zhang, H. Wang, D.P. Wilkinson, *A review of anode catalysis in the direct methanol fuel cell*, *J. Power. Sources* 155 (2006) 95–110.
- [22] X. Li, A. Faghri, *Review and advances of direct methanol fuel cells (DMFCs) part I: design, fabrication, and testing with high concentration methanol solutions*, *J. Power. Sources* 226 (2013) 223–240.
- [23] G.H. An, D.Y. Lee, H.J. Ahn, *Tofu-derived carbon framework with embedded ultrasmall tin nanocrystals for high-performance energy storage devices*, *J. Alloys Compd.* 722 (2017) 60–68.
- [24] D.Y. Lee, G.H. An, H.J. Ahn, *High-surface-area tofu based activated porous carbon for electrical double-layer capacitors*, *J. Ind. Eng. Chem.* 52 (2017) 121–127.
- [25] G.H. An, H.J. Ahn, W.K. Hong, *Electrochemical properties for high surface area and improved electrical conductivity of platinum-embedded porous carbon nanofibers*, *J. Power. Sources* 274 (2015) 536–541.
- [26] M.K. Jeon, K.R. Lee, H.J. Jeon, P.J.M. Ginn, K.H. Kang, G.I. Park, *Quaternary Pt₂Ru₁Fe₁M₁/C (M=Ni, Mo, or W) catalysts for methanol electro-oxidation reaction*, *Kor. J. Chem. Eng.* 32–2 (2015) 206–215.
- [27] S.H. Gage, C. Ngo, V. Molinari, M. Causa, R.M. Richards, F.S. Gentile, S. Pylypenko, D. Esposito, *Strong Metal–Support interactions of TiN– and TiO₂–Nickel nanocomposite catalysts*, *J. Phys. Chem. C* 122 (2018) 339–348.
- [28] G.H. An, D.Y. Lee, H.J. Ahn, *Vanadium nitride encapsulated carbon fibre networks with furrowed porous surfaces for ultrafast asymmetric supercapacitors with robust cycle life*, *J. Mater. Chem. A* 5 (2017) 19714–19720.
- [29] G.H. An, D.Y. Lee, H.J. Ahn, *Tunneled mesoporous carbon nanofibers with embedded ZnO nanoparticles for ultrafast lithium storage*, *ACS Appl. Mater. Interfaces* 9 (2017) 12478–12485.
- [30] G.H. An, D.Y. Lee, Y.J. Lee, H.J. Ahn, *Ultrafast lithium storage using antimony-doped tin oxide nanoparticles sandwiched between carbon nanofibers and a carbon skin*, *ACS Appl. Mater. Interfaces* 8 (2016) 30264–30270.
- [31] G.H. An, E.H. Lee, H.J. Ahn, *Well-dispersed iron nanoparticles exposed within nitrogen-doped mesoporous carbon nanofibers by hydrogen-activation for oxygen-reduction reaction*, *J. Alloys Compd.* 682 (2016) 746–752.